ELSEVIER

Polymer 41 (2000) 5909–5919

polymer

On the stress, strain and energy density repartitions in particle-reinforced elastomer networks

A. Burr*, L. Monnerie

PCSM-ESPCI UMR 7615, 10 rue Vauquelin, F-75231 Paris Cedex 05, France

Received 26 July 1999; accepted 3 November 1999

Abstract

In this paper, the Distributed Generalized Self-Consistent homogenization model is used to analyze the stress, strain and free energy density distributions in particle-reinforced elastomers. This information is crucial to bring out guidelines to understand the mechanism of deformation in heterogeneous materials such as filled elastomers. An application of the Distributed Generalized Self-Consistent Scheme is fully analyzed in the case of a tension test for several arrangements of particles inside the elastomer matrix.

Keywords: Filled elastomers; Homogenization; Physico-mechanical behavior

1. Introduction

The motivation for this study was initiated by the interest of relating the local physico-chemical properties of a filled elastomer network to its mechanical properties using the Distributed Generalized Self-Consistent homogenization model. Moreover, this new approach can predict the relations between the morphology of a filled elastomer network (microscopic arrangement of particles), the local mechanical behavior of the constituents and the macroscopic mechanical behavior. The aim of this note is to provide a methodology from the observation of the material to its complete mechanical characterization.

Classical homogenization techniques can only describe the composition of material with the volume fraction. Therefore, the information that they can provide is limited. In order to keep track of the morphology of the filled elastomer, the Concentration Distribution Function (CDF) is introduced to model the variation of the local concentration.

The area of investigation of this paper is limited to elastomer reinforced by non-percolating particles. But, all concepts that are presented here can be extended to all types of particle-reinforced composites.

2. Material observations

Material observations are necessary to reveal the organization of the particles inside the elastomer matrix composite. Now-a-days, the means of observation are still limited to two-dimensional pictures since three-dimensional imaging is not yet available. Transmission Electron Microscope (TEM) pictures have a good resolution, but they are taken on a thin film of the material. The investigation of the fine structure can be made by Atomic Force Microscopy (AFM) with the tapping mode and phase contrast directly on the surface of the specimen. In order to observe a representative morphology, the area of observation should be greater than hundred times the size of the particle.

One of the important information pointed out by these observations is the notion of local concentration. In Fig. 1, there are locations where the particles are very close together, with very little amount of matrix and other places where a large amount of matrix surrounds some isolated particles. This means that the local concentration is not uniformly distributed in the material. In order to account for this dispersion, the local concentration will be modeled by a CDF. It is worth noting that a local volume concentration can range from 0 up to 0.74 even in a composite containing 0.20, in volume, of nanoparticles of filler.

2.1. Notion of local concentration

In a general formalism, the local concentration defines the

* Corresponding author. Fax: +33-1-40-79-4686.
E-mail address: alain.burr@espci.fr (A. Burr).

0032-3861/00/$ - see front matter
PII: S0032-3861(99)00816-2

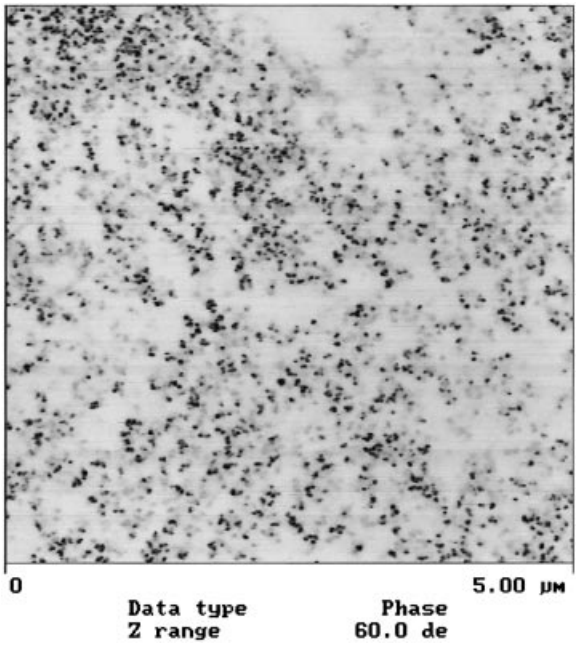

Fig. 1. Atomic force microscope pictures of an elastomer reinforced by nanoparticles of silicate [1].

composition of a composite upon a given "area". The difficult point of this concept is to give a clear definition of the "area" which is representative.

For particle reinforced composites, the local concentration, c, is related to a composite sphere, and defined as the ratio of the volume of the particle over the composite sphere (Fig. 2).

The next step is to build the CDF. As there are no percolating particles, each composite sphere is directly counted to their corresponding local volume fraction, c:

$$c = \left(\frac{r_p}{r_{cs}}\right)^3 \tag{1}$$

where r_p is the radius of the particle and r_{cs} the radius of the composite sphere.

Percolating structure needs more attention because both constituents are continuous. They can be considered as two inter-connected phases. Therefore, their respective proportions are reported at 0 and 1.00 volume fraction of particles, which means that matrix and percolating particles are mixed together without any order.

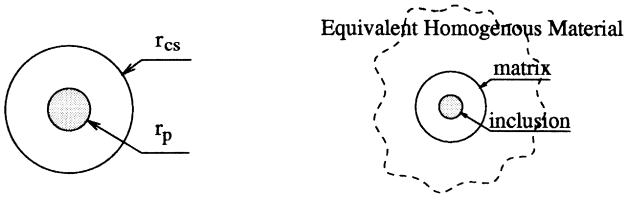

Fig. 2. Definition of the local concentration and generalized self-consistent scheme.

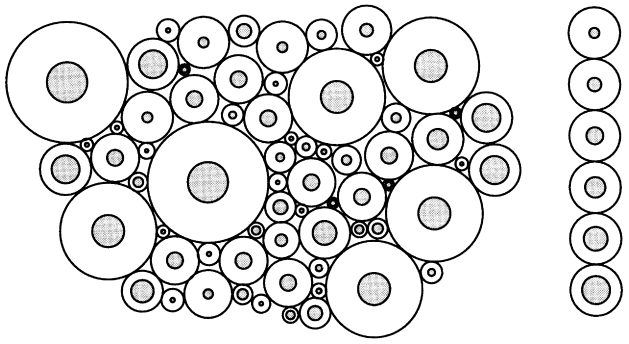

Fig. 3. Representation of the local concentration distribution in the material.

2.2. Introduction of the concentration distribution function

Any particle-reinforced composite material can be considered as a gathering of composite spheres (Fig. 3). All composite spheres are counted, on a distribution graph, at their specific concentration, c. Formally, this discrete representation is continuously prolongated to a function. The description of the topology of the composite is given by a CDF, $\phi[c]$ (Fig. 4).

The average value of the CDF is by definition the value of the volume fraction of particles:

$$f_v \equiv \int_0^1 \phi[c]c \, dc \tag{2}$$

3. Bases of the mechanical modelization

According to the material observation, homogenization seems to be a good candidate to derive mechanical properties of this kind of composite. Since the constituents are well defined, in terms of their local mechanical properties and in terms of repartition inside the composite, it is possible to derive the macroscopic properties and local stress, strain and energy density fields. But some simplifications need to be done and will be presented next.

The mechanical behavior of the nanoparticles will be

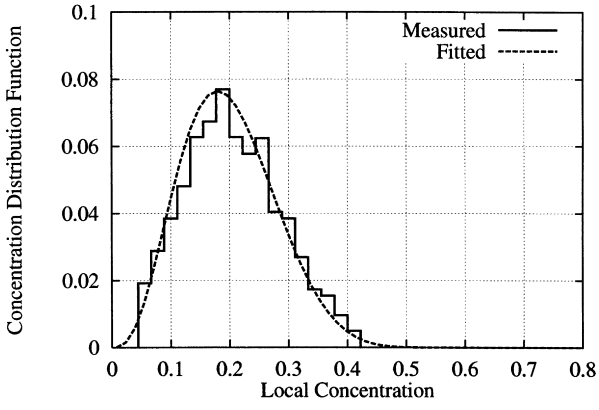

Fig. 4. Graph of a CDF [1].

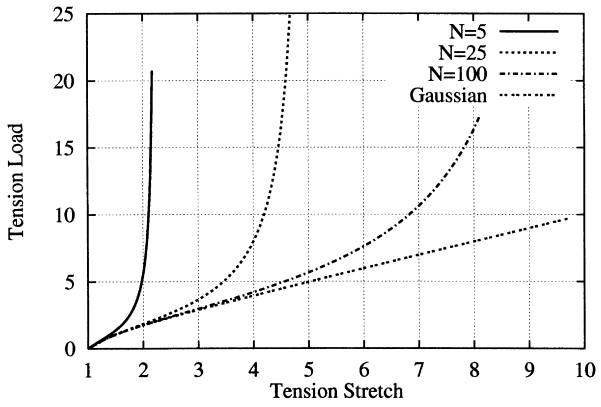

Fig. 5. Load displacement graph of a network of chains for different values of number of links, *N*.

considered the same as the bulk material. The mechanical behavior of the matrix is derived from the behavior of a single macromolecular chain by a homogenization over the elastomer network. It is assumed that the interface between the particles and the matrix cannot be damaged, which means that the adhesion is perfect.

The next point is to choose the more appropriate homogenization scheme. From the AFM observations (Fig. 1), the particles are surrounded by the continuous matrix. The Generalized Self-Consistent Scheme [2] (Fig. 3) is a good candidate to catch the feature of a single continuous constituent in terms of macroscopic properties and averages of local strain, stress and free energy density fields. The limitation of this approach is linked to the use of a single-composite sphere, which concentration is equal to the macroscopic volume fraction of particles. A further step has been done by using the Generalized Self-Consistent Scheme with distribution of local concentration [3–5]. This scheme can model the dispersion of the local concentration by considering a CDF, as defined above.

According to the material observation, the investigated field is limited to the case of non-mechanically percolating particles. It means that the organization of particles is not able to carry load on their own, but there is still a load transfer from the particles to the matrix.

3.1. Constitutive equations of the particles

The mechanical behavior of the rigid particles is assumed to be linear elastic and isotropic. The expression of the free energy density, $\rho\psi_p$, has the classical form:

$$\rho\psi_p[\epsilon_p] = G_p e_p : e_p + \frac{1}{2}K_p\epsilon_{pv}^2 \tag{3}$$

where ρ is the density of the particles, ϵ_p the total strain tensor, e_p its deviatoric part and ϵ_{pv} its volume part. G_p is the shear modulus and K_p is the bulk modulus. All these quantities are related to the particles, e.g. the subscript p.

The expression of the stress tensor, σ_p, is given by:

$$s_p = 2G_p e_p \qquad p_p = K_p\epsilon_{pv} \tag{4}$$

where p_p is the pressure and s_p the deviatoric part of the stress tensor, σ_p.

3.2. Constitutive equations of the elastomer network

In an elastomer-like material, the conformation of the flexible long-chain macromolecules changes continuously, e.g. Brownian motion. According to statistical thermodynamics, the number of conformations defines the entropy of the elastomer, and is modified with the applied stretch.

Due to the stretching limit of a polymer chain, at high stretch, the statistics of the chain does not follow a Gaussian distribution of the end-to-end chain vector, *r*. According to the work of Kuhn and Grün [6,7], the expression of the entropy, *s*, of one freely jointed single chain, made of *N* elementary links of length *b*, is:

$$\Delta s = -\mathrm{k}N\left(\frac{r}{Nb}\beta + \ln\left[\frac{\beta}{\sinh[\beta]}\right]\right) \tag{5}$$

where $\beta = L^{-1}(r/Nb)$ is the solution of:

$$\frac{r}{Nb} = \coth[\beta] - \frac{1}{\beta} = L[\beta] \tag{6}$$

with *L* representing Langevin's function. k is Boltzmann's constant, *r* the end-to-end chain vector, $r_0 = b\sqrt{N}$, the average end-to-end distance of the undeformed chain.

When $r \le (Nb/3)$, the expression of the entropy (Eq. (5)) reduces to:

$$\Delta s = -\frac{3}{2}\mathrm{k}\frac{r^2}{Nb^2} = -\frac{3}{2}\mathrm{k}\frac{r^2}{r_0^2} \tag{7}$$

The tension on a single chain of *N* elementary links with the end-to-end chain vector, *r*, is obtained by the derivation of the entropy, Δs, with respect to *r*.

At the network level the model of Voigt [8], uniform (constant) strain across all chains in the elastomer, is applied to compute the free energy density. This means that the displacement of the cross-linking points is proportional to the macroscopic displacement. It is also assumed that the entropy of the network is equal to the sum of the entropy of the individual chains.

Under tension, the load, *f*, displacement relation of a network of *n* chains per unit volume, each with *N* elementary links, is given by:

$$f = n\mathrm{k}T\frac{N^{1/2}}{3}\left(L^{-1}\left[\frac{\lambda_t}{N^{1/2}}\right] - \frac{1}{\lambda_t^{3/2}}L^{-1}\left[\frac{1}{N^{1/2}\lambda_t^{1/2}}\right]\right) \tag{8}$$

where λ_t is the simple extension ratio in tension and *T* the absolute temperature.

The first-order approximation of expression in Eq. (8) corresponds to the Gaussian approach (Fig. 5) which gives:

$$f = n\mathrm{k}T\left(\lambda_t - \frac{1}{\lambda_t^2}\right) \tag{9}$$

The tension curves are shown on Fig. 5 for Gaussian and

non-Gaussian behaviors with different values of elementary links, N.

For multi-axial loading condition, in isovolume deformation conditions, $\lambda_1\lambda_2\lambda_3 = 1$, of a network of non-Gaussian chains, the entropic elasticity of this network gives an expression of the free energy density, $\rho\psi_s$:

$$\rho\psi_s[\lambda] \equiv -\mathrm{k}Ts[\lambda] = -\mathrm{k}T(s[\lambda_1] + s[\lambda_2] + s[\lambda_3])$$
$$= -\mathrm{k}T\left(s[\lambda_1] + s[\lambda_1] + s\left[\frac{1}{\lambda_1\lambda_2}\right]\right) \quad (10)$$

where λ_i are the principal values of the isovolume stretch tensor of the network, λ. It is worth noting that, the isovolume condition leads to an expression of the free energy density, $\rho\psi_s$, which is only function of two of them, which are chosen to be λ_1 and λ_2. The second equality corresponds to the fact that both free energy density and entropy density are state functions, which means that their expression is not path dependent.

It leads to:

$$\rho\psi_s[\lambda] = n\mathrm{k}T\frac{N^{1/2}}{3}\left(\lambda_1\beta_1 + \ln\left[\frac{\beta}{\sinh[\beta_1]}\right] + \lambda_2\beta_2\right.$$
$$\left. + \ln\left[\frac{\beta_2}{\sinh[\beta_2]}\right] + \lambda_3\beta_3 + \ln\left[\frac{\beta_3}{\sinh[\beta_3]}\right]\right) \quad (11)$$

where β_i is the solution of the inverse Langevin's function (Eq. (6)) for their respective λ_i.

This latter expression can be reduced to a Gaussian behavior with the following expression for the free energy density:

$$\rho\psi_s[\lambda] = n\mathrm{k}T\left(\lambda_1^2 + \lambda_2^2 + \frac{1}{\lambda_1^2\lambda_2^2} - 3\right) \quad (12)$$

The internal energy density contribution gives the hydrostatic part of the free energy density, $\rho\psi_v$:

$$\rho\psi_v[\epsilon_v] = \tfrac{1}{2}K\epsilon_v^2 \quad (13)$$

where K is the bulk modulus and ϵ_v the volume strain.

By combining the two parts of the free energy density, the constitutive equation of the matrix can be derived. The expression of the nominal (engineering or Piola-Kirchoff 2) stress tensor, σ, is obtained by the derivation of the total free energy density, $\rho\psi$, with respect to the total strain, ϵ:

$$\sigma = \rho\frac{\partial(\psi_s + \psi_v)}{\partial\epsilon} = \rho\frac{\partial\psi}{\partial\epsilon} \quad (14)$$

where $\lambda = 1 + \epsilon$.

By applying Eq. (14) to Eqs. (11) and (13), the components of the real stress tensor (Cauchy), σ_1 and σ_2 are given by:

$$\sigma_1 = n\mathrm{k}T\left(\lambda_1^2 - \frac{1}{\lambda_1^2\lambda_2^2}\right)Q_1[\lambda_1, \lambda_2]$$
$$\sigma_2 = n\mathrm{k}T\left(\lambda_2^2 - \frac{1}{\lambda_1^2\lambda_2^2}\right)Q_2[\lambda_1, \lambda_2] \quad (15)$$

which can be approximated, as suggested by Bueche and Halpin [9,10], by:

$$\sigma_1 = n\mathrm{k}T\left(\lambda_1^2 - \frac{1}{\lambda_1^2\lambda_2^2}\right)\frac{1 - \lambda_{\lim}^2}{\lambda_1^2 - \lambda_{\lim}^2}$$
$$\sigma_2 = n\mathrm{k}T\left(\lambda_2^2 - \frac{1}{\lambda_1^2\lambda_2^2}\right)\frac{1 - \lambda_{\lim}^2}{\lambda_2^2 - \lambda_{\lim}^2} \quad (16)$$

to account for the limit average stretch of the polymer chain network, $\lambda_{\lim}$, and the pressure, p, has the classical expression:

$$p = K\epsilon_v \quad (17)$$

A first-order approximation of the stress relations (Eq. (15)) gives the expression of the Gaussian relations:

$$\sigma_1 = n\mathrm{k}T\left(\lambda_1^2 - \frac{1}{\lambda_1^2\lambda_2^2}\right) \qquad \sigma_2 = n\mathrm{k}T\left(\lambda_2^2 - \frac{1}{\lambda_1^2\lambda_2^2}\right) \quad (18)$$

In small strain conditions, e.g. $\epsilon < 50\%$ for a filled elastomer, the macroscopic behavior is supposed to be isotropic and remain isotropic during the loading, because there is no strong reorganization of the topology of the particles.

The difficulties in modeling the behavior of reinforced elastomer with homogenization are first related to the non-linear elasticity of the elastomer and secondly correlated to finite transformations, e.g. geometrically non-linear.

Non-linear behavior of the elastomer composite is equivalent to the linear behavior of a comparison composite, e.g. tangent or secant moduli [11–13]. For metals, other authors [14–16] have proposed different equivalent values of the strain or stress for the evaluation of the evolution law of the plastic deformation. But in general, from a technical point of view, they are all leading to the definition of a non-local constitutive equation [17] of the material.

For elastomers, the elastic part of the behavior is non-linear. In this study, the choice of the equivalent value of the stretch tensor, λ_{eq}, is taken equal to the average value in the matrix of each composite sphere:

$$\lambda_{eq} = \left(\sqrt{\frac{1}{V_m}\int_{\Omega_m}\lambda_{1m}\,dV}\sqrt{\frac{1}{V_m}\int_{\Omega_m}\lambda_{2m}\,dV}\frac{1}{V_m}\int_{\Omega_m}\lambda_{3m}\,dV\right)^{-1} \quad (19)$$

Nevertheless, another possibility mentioned by Ponte

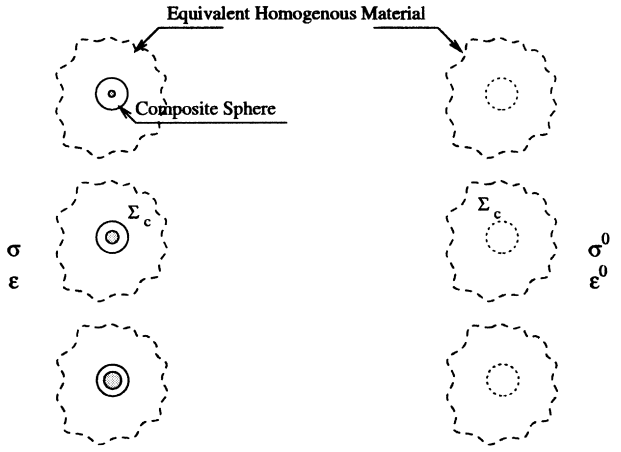

Fig. 6. Equivalent inclusion modelization applied to the generalized self-consistent scheme with the introduction of local concentration.

Castaneda [18] is based upon the second invariant:

$$\lambda_{eq} = \frac{1}{V_m}\int_{\Omega_m}\sqrt{\frac{1}{2}\lambda_m : \lambda_m}\,dV$$

$$= \frac{1}{V_m}\int_{\Omega_m}\sqrt{\frac{1}{6}((\lambda_{1m}-\lambda_{2m})^2+(\lambda_{1m}-\lambda_{3m})^2+(\lambda_{2m}-\lambda_{3m})^2)}\,dV$$

$$= \frac{1}{V_m}\int_{\Omega_m}\sqrt{\frac{1}{6}((\epsilon_{1m}-\epsilon_{2m})^2+(\epsilon_{1m}-\epsilon_{3m})^2+(\epsilon_{2m}-\epsilon_{3m})^2)}\,dV \quad (20)$$

where λ_m is the isovolume stretch tensor of the matrix, and λ_{1m}, λ_{2m}, λ_{3m} their principal values, and ϵ_m is the isovolume strain tensor of the matrix, and ϵ_{1m}, ϵ_{2m}, ϵ_{3m} their principal values.

3.3. Homogenization procedure

The objectives of this subsection are to recall the bases of the homogenization technique [19] and to introduce the distributed homogenization scheme.

Eshelby's formulas are useful results in elasticity theory in the heterogeneous material analysis [20,21]. The formulas that he derived reduce the usual integrations of elastic energy to a particular type of surface integration. For the self-consistent approach with the distribution of local concentration, $\emptyset[c]$, the energy equivalence relationship is reduced to:

$$\int_0^1\left(\frac{1}{2}\int_{\Sigma_c}(T\cdot u^0 - T^0\cdot u)\,ds\right)\emptyset[c]\,dc = 0 \quad (21)$$

where Σ_c is the surface of the composite sphere of local concentration c, T^0 and u^0 are, respectively, the stress and displacement acting on the homogeneous medium, and T and u are, respectively, the stress and displacement at the same point in the medium containing the inclusion (Fig. 6).

Many authors have used this expression to estimate effective moduli of the equivalent homogeneous medium (see for e.g. Refs. [22–25]). But only in some particular cases, exact solutions for the effective moduli can be obtained (see for e.g. Refs. [2,26–29]) otherwise it is possible to derive bounds of the effective moduli [3,8,30–32], and in some specific cases non-linear behavior [33,34]. The next paragraph will present an overview of the concept of equivalent homogeneity [35] and its implications on the mechanical analysis.

In practice, there is scale at which all materials are heterogeneous. The heterogeneity can occur, either as a continuous variation of properties with position or as an abrupt change in properties across interface. According to TEM or AFM observations, in this work, only the latter case will be considered, and the field of investigation is reduced to homogenization of spherical inclusions. Furthermore, the Representative Elementary Volume, V_{REV}, over which the properties are averaged, is of a dimension much larger than a characteristic volume, V_{cs} (Fig. 7), e.g. the volume of a composite sphere. Consequently, at the representative level, the material is idealized as being homogeneous.

The topology of the particles in the elastomer is dictated by the condition of mixing and the affinity of the particles to form aggregates. The consequence resulting from the processing stage is that the nanostructure of the reinforced elastomer can be controlled. But the macroscopic mechanical behavior of the reinforced elastomer is different. In order to have some ideas on that behavior, it is necessary to introduce the information on the topology of the particles in the elastomer. In this approach, the topology will be characterized by the local concentration (Figs. 2 and 3).

The treatment is based upon the Generalized Self-Consistent Scheme [2] with consideration of the CDF. The solutions of a single composite sphere made of two layers are now applied to a gathering of composite spheres [36]. Each composite sphere is defined by its local concentration, and its occurrence in the material is described through a CDF. The derivation of the strain and stress fields follow the expressions given by Christensen and Lo [2]. The only difference corresponds to the application of the energy equivalence because of the presence of a distribution of composite spheres with different local concentration.

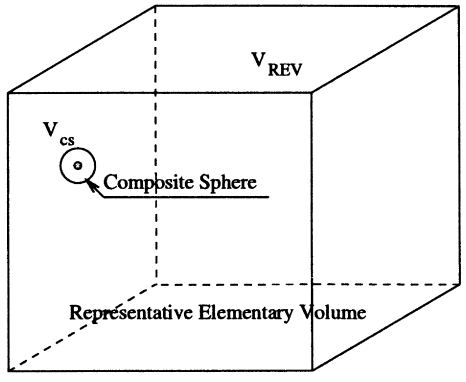

Fig. 7. Concept of characteristic length and length scale.

Table 1
Value of the moduli of the matrix and nanoparticles

Properties	Elastomer	Nanoparticles
Young's modulus (E)	7 MPa	60 GPa
Poisson's ratio (ν)	0.49	0.2
Limit stretch (λ_{lim})	1.5	–

In this more general case, the energy condition (Eq. (21)) is integrated over all composite spheres, multiplied by their respective weight in terms of their occurrence in the material, e.g. with the CDF.

4. Analyses of the results

Typical values of the behavior of the elastomer and the nanoparticles are reported in Table 1. The area of investigation is limited, at the macroscopic level, to the stress–strain curves for tension tests, at the local level, to the strain, stress and free energy density fields.

4.1. Effect of Gaussian and non-Gaussian constitutive equations of the elastomer matrix

Tension tests has been performed upon coupons for different volume fractions of particles. The reinforcement obtained by the addition of particles in the elastomer has two different origins. The first one is directly related to the presence of hard spheres in a soft matrix (Fig. 8). The second one, which is manifested with a non-Gaussian behavior of the elastomer matrix, is due to increase of stiffness of the matrix, as the load of the matrix increases (Fig. 9).

The graphs shown in Fig. 9 deal with a composite system containing a mean volume fraction of particles equal to 0.30, with the CDF given in Fig. 10. In order to respect the close packing of monodispersed size of spheres, e.g. 0.64, the value of the CDF has been taken equal to zero for all concentration upon this limit. The result of the computation using a Gaussian constitutive equation for the pure elastomer (curve (a) in Fig. 9), whereas the curve (b) of Fig. 9 is obtained from Langevin's constitutive equation. It

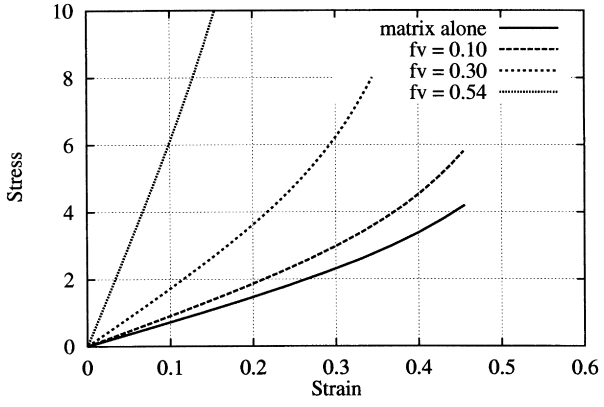

Fig. 8. Effect of the volume fraction of particles on a tension test.

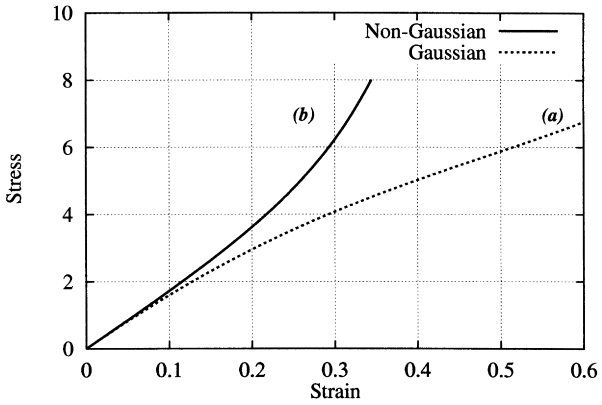

Fig. 9. Simulations of a tension tests on a particle reinforced elastomer (mean volume fraction of particles, $f_v = 0.30$).

is worth noting that there is a significant increase of the stress (100%) at a strain of 40%. When the volume fraction of the particles increases, the effect of the non-Gaussian behavior of the elastomer occurs at a lower strain (Fig. 8). The latter remarks are only valid until there is no decohesion at the interface between the particles and the matrix.

All the results presented in the following paragraphs correspond to the average value in the matrix of stress, strain and free energy fields. The stress and strain fields are written in terms of the intensity factors of the deviatoric and hydrostatic decompositions of their respective tensor. The free energy field is described by its density, which gives a good feeling of its unit volume repartition in the matrix, and a distribution function, which characterizes the amount of volume in the matrix at the same energy level. In each of the following figures, figure (a) refers to Gaussian and figure (b) to non-Gaussian constitutive equation of the elastomer matrix. Moreover, the "elastic" case refers to linear approximation of the constitutive equation of the matrix, which physically corresponds to an applied load leading to zero.

The strain intensity factor, ϵ_{if}, is defined as:

$$\epsilon_{if} \equiv \frac{\dfrac{1}{v_m}\displaystyle\int_{\Omega_m} \epsilon_m \, dv}{\epsilon^{\infty}} \tag{22}$$

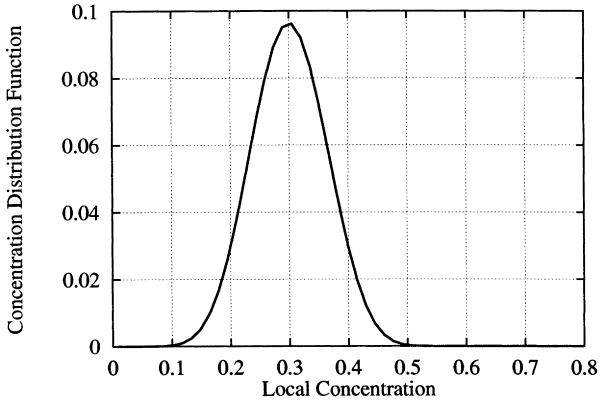

Fig. 10. Representation of the CDF.

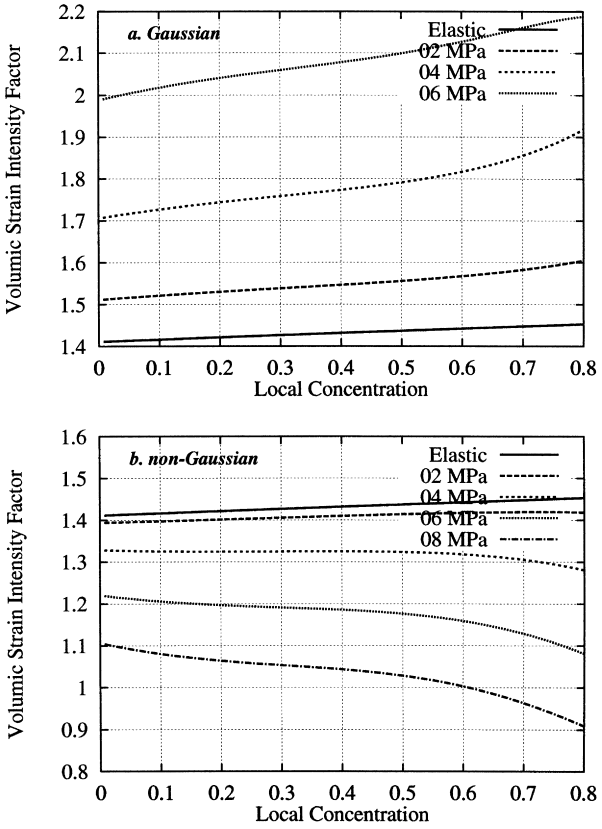

Fig. 11. Volume strain intensity factor in the elastomer.

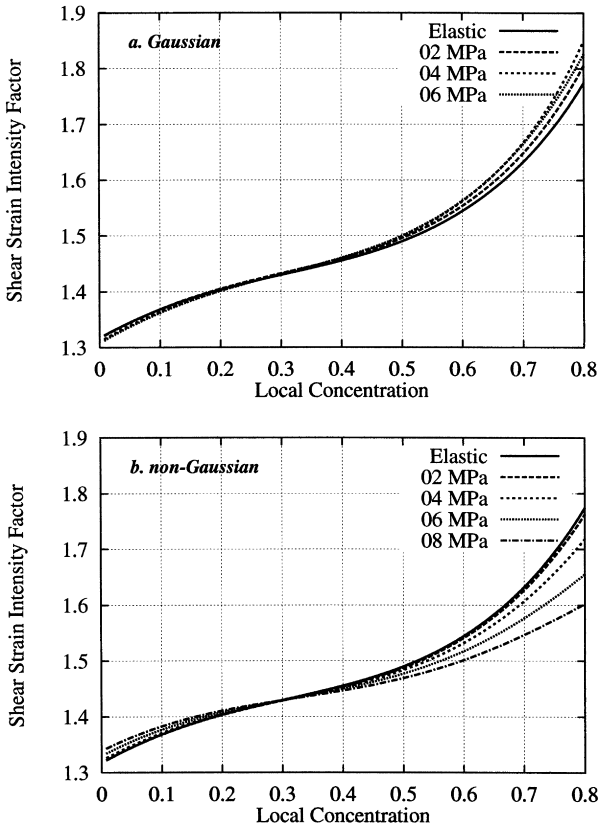

Fig. 12. Shear strain intensity factor in the elastomer.

where ϵ_m is the strain tensor of the elastomer, Ω_m the part of the matrix in a given composite sphere, which has a volume, v_m, and ϵ^∞ the applied far-field strain tensor.

The profile of the repartition of the volume strain intensity factor (Fig. 11) is rather uniform in both cases. As the load increases, the mean value of the repartition decreases and its profile becomes less uniform with the increasing load for Langevin's constitutive equation of the elastomer. On the contrary, its mean value increases with the load for the Gaussian case.

The shear strain intensity factor is presented in Fig. 12. It is higher at the higher local concentration of particles for any load value. Such a profile remains rather constant with increasing load for the Gaussian behavior of the matrix. For the non-Gaussian regime, the effect of the loading appears completely different: at high local concentration, there is a quite significant decrease of the shear strain intensity factor (10% at 8 MPa), whereas only a slit increase occurs at low local concentration. Moreover, at a local concentration around the mean volume fraction, there is no load effect. These results show gradual shear strain redistribution between the composite spheres of different concentration of particles.

The definition of the stress intensity factor, σ_{if}, is given by:

$$\sigma_{if} \equiv \frac{\dfrac{1}{v_m}\displaystyle\int_{\Omega_m} \sigma_m \, dv}{\sigma^\infty} \tag{23}$$

where σ_m is the strain tensor of the elastomer and σ^∞ the applied far-field stress tensor. The representation of the result has been divided in the hydrostatic part (pressure) and the deviatoric part of the stress.

For the two matrix behaviors, the repartition of the pressure intensity factor (Fig. 13) is rather uniform, and becomes less uniform with increasing load. Similarly to what is obtained for the volume strain intensity factor, increasing the load leads to opposite changes of the hydrostatic stress intensity factor between the Gaussian and the non-Gaussian behavior of the matrix. As regards the shear stress intensity factor (Fig. 14), there is a great difference between the two matrix responses. Indeed, for the Gaussian matrix behavior, the profile with local concentration looks like the one obtained for the corresponding shear strain intensity factor, and does not depend on the load. It is quite different with the non-Gaussian behavior of the matrix, for which similar profiles are noticed between shear strain and stress intensity factors, but the effects of increasing load are completely different. Both for low and high local concentration, large changes with loading result (10% at 8 MPa). They occur in opposite directions, with a fixed point at the local concentration equal to the mean volume fraction. Consequently, the distribution of the shear stress intensity factor through the composite spheres of various concentration becomes wider and wider by increasing the load.

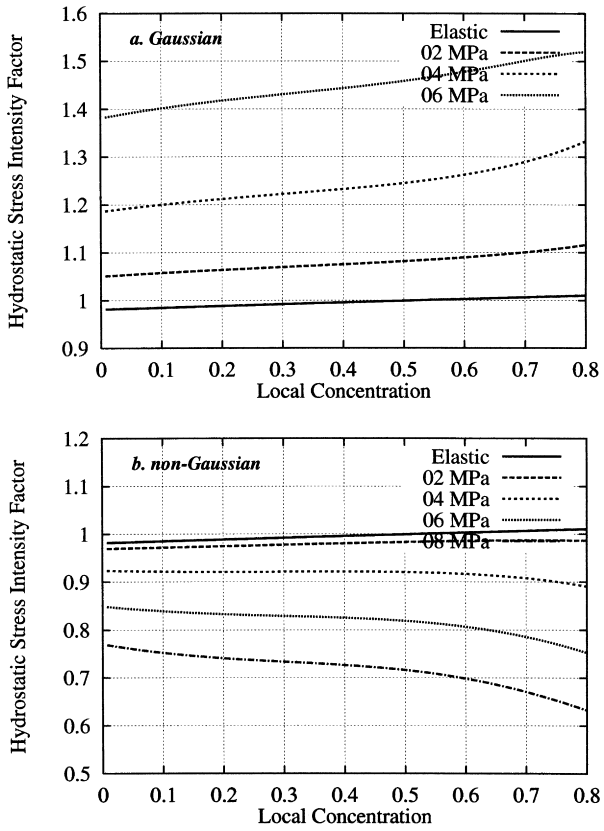

Fig. 13. Hydrostatic stress (pressure) intensity factor in the elastomer.

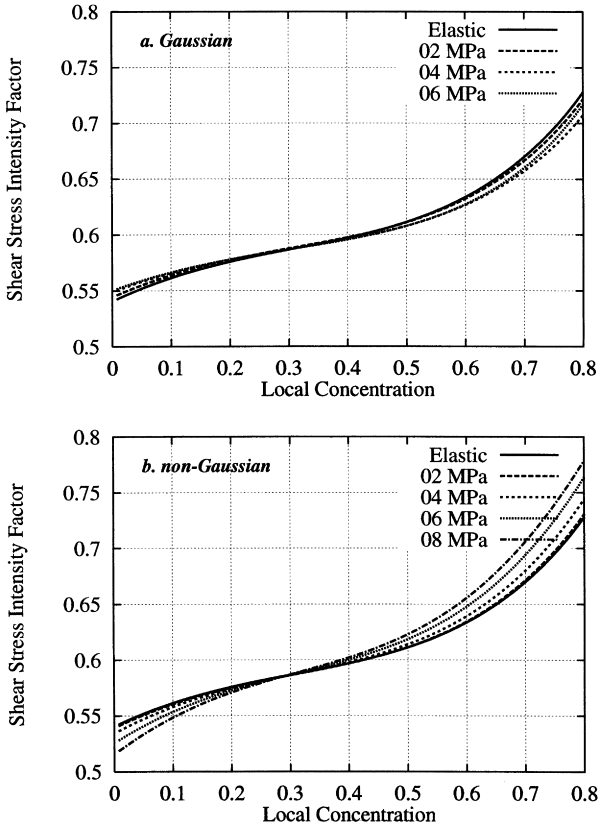

Fig. 14. Deviatoric stress (shear) intensity factor in the elastomer.

For each value of the local concentration, the free energy density of the matrix, ψ_m, is defined as

$$\psi_m \equiv \frac{1}{2v_m}\int_{\Omega_m} \sigma_m : \epsilon_m \, dv \tag{24}$$

The free energy density is shown in Fig. 15. It is worth to point out that the absolute values of the free energy density at a given stress level cannot be compared between the Gaussian and the non-Gaussian behaviors of the matrix as shown in Fig. 9; higher free energy densities are stored in the Gaussian case, due to the larger strain required to achieve the same stress. Any way, in both cases, the free energy density of the matrix is located at high local concentration.

The free energy distribution function is defined as:

$$\Phi_m(c) \equiv (1-c)\phi(c) \times \frac{\dfrac{1}{2v_m(c)}\displaystyle\int_{\Omega_m} \sigma_m : \epsilon_m \, dv}{\displaystyle\int_0^1 (1-c)\phi(c)\left(\frac{1}{2v_m(c)}\int_{\Omega_m} \sigma_m : \epsilon_m \, dv\right) dc} \tag{25}$$

The free energy distribution (Fig. 16) does not depend at all on the Gaussian or non-Gaussian character of the behavior of the elastomer matrix. Indeed, it is directly controlled by the corresponding CDF, and exactly reflects its shape. The absolute value of the free energy is higher for Gaussian than non-Gaussian behavior of the matrix, as a consequence of what has been described here above for the free energy density.

4.2. Effect of the concentration distribution function

For the non-Gaussian behavior of the matrix, we investigated the effect of the shape of the CDF on either the macroscopic stress–strain relation, or the local strain, stress and free energy fields. For a volume fraction equal to 0.30, we have looked at the various CDFs shown in Fig. 17, in addition to the previous one (Fig. 10). Each CDF is labeled from 1 to 4.

Tension tests have been performed by using the four different CDFs. The results shown in Fig. 18 in terms of the stress–strain curves are the same. This result is rather surprising because the self-consistent approach accounts for the strain (or stress) coupling between the different composite spheres through the equivalent homogeneous surrounding material.

From a practical point of view, only the volume fraction of particles is the relevant parameter, which means that the tension curve can be derived by using a standard model, e.g. Generalized Self-Consistent [2], extended to non-linear

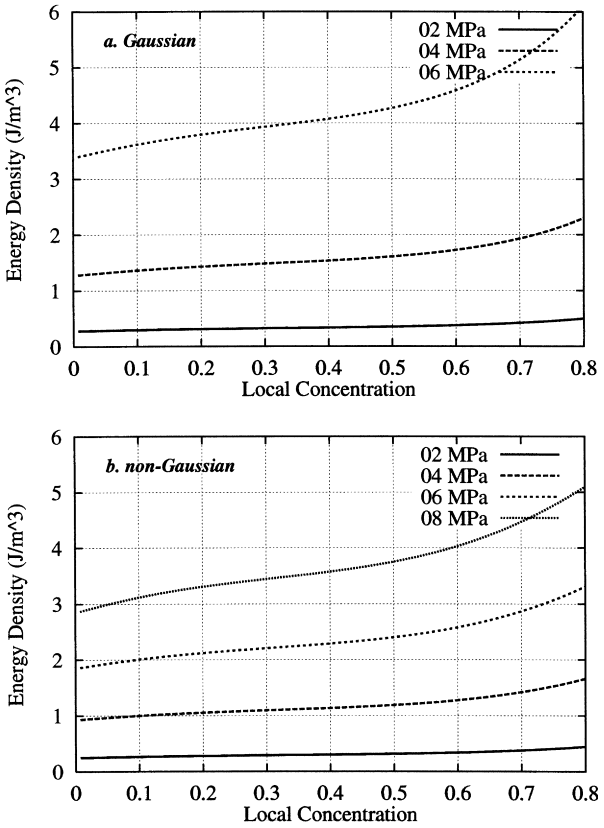

Fig. 15. Free energy density of the elastomer.

behavior. Nevertheless, this approach gives finer information on the different fields acting in the heterogeneous material, which can be exploited to study molecular mechanisms. Other investigations on different non-percolating morphologies of particles lead to the same conclusion. It is interesting to look at the influence of different CDFs on the local fields. For example, the shear strain intensity factor (Fig. 19) increases slightly when the CDF is getting wider. Similarly, the free energy density (Fig. 20) is quite independent of the arrangement of particles in the

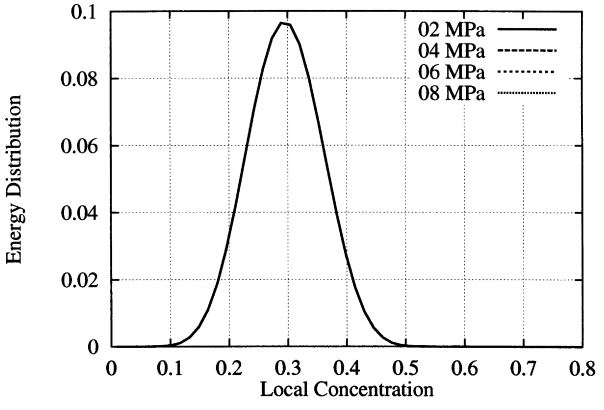

Fig. 16. Free energy distribution function of the elastomer.

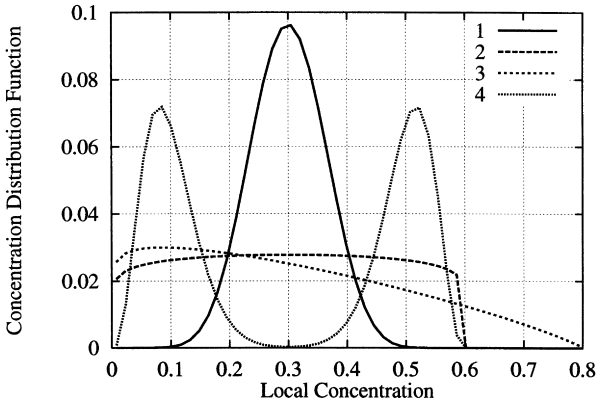

Fig. 17. Set of CDFs.

elastomer matrix and seems to be directly dictated by the load level (8 MPa).

5. Conclusion

The previous sections have shown that the Distributed Generalized Self-Consistent model is able to derive macroscopic stress–strain relation for any loading condition, and also to bring out the local stress, strain and energy density fields in a heterogeneous material. The advantage of this model is the quick answer and the simplicity of use. At this stage, with this analytic approach, it is only possible to study the behavior under the hypothesis of small strains, e.g. up to $\epsilon < 50\%$.

This limitation is first due to large transformation, which changes the shape of the composite sphere to a composite ellipsoid. Secondly, the treatment of the non-linear behavior, and especially the introduction of the composite of comparison cannot yet be analytically solved. For a classical constitutive equation, e.g. local constitutive equation, some authors [37] have gone through Finite Element simulations, but these computations are time consuming because the non-linear behavior is step by step updated. Furthermore,

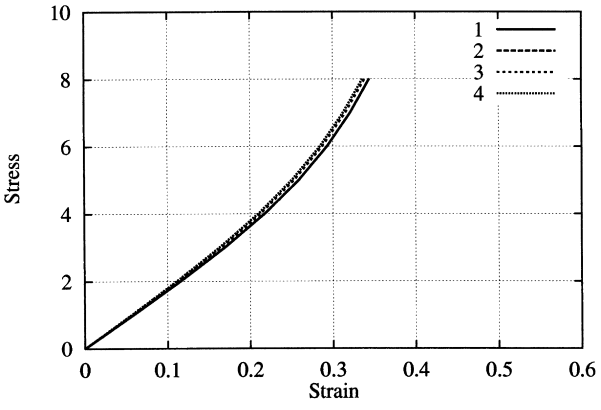

Fig. 18. Tension test for different CDFs.

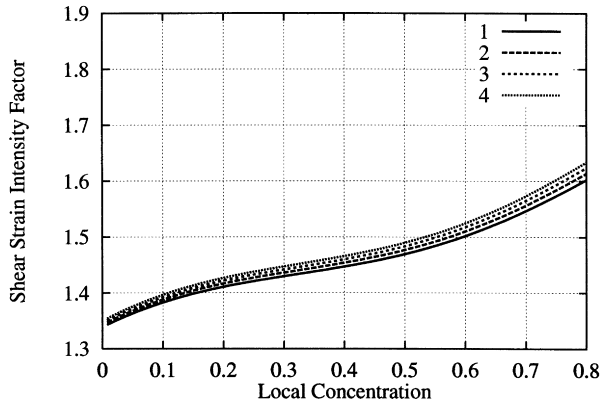

Fig. 19. Shear strain intensity factor for different distribution function.

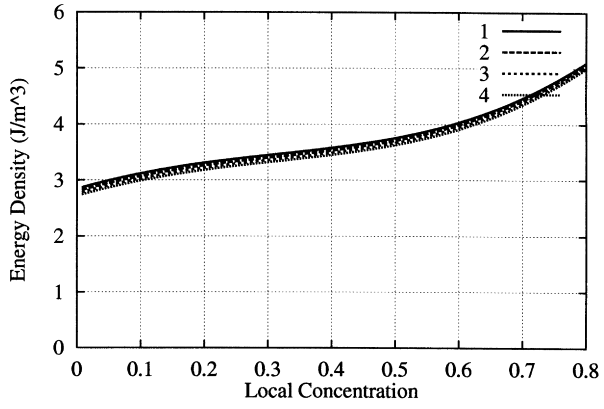

Fig. 20. Free energy density of the matrix for different CDFs.

to account for the local concentration, e.g. the Concentration Distribution Function, Finite Element approach does not appear to be a good candidate, because it will cost more computer time and, moreover, the solution might not be unique. To overcome this difficulty, in this work, the behavior of the elastomer has been considered as non-local, which means that it depends upon the average of strain field of the matrix of each composite sphere. As a consequence, the matrix of each composite sphere can follow its own history.

The principal results have been obtained by considering a tension test. They have shown that the local fields (strain or stress) depend quite significantly on the local concentration of particles, meaning that the response of the composite material is heterogeneous.

The effect of the stress load level depends on the considered local field. A major influence is observed between a Gaussian and a non-Gaussian character of the constitutive equation of the elastomer matrix. In most cases, the composite spheres of high concentration show the higher sensitivity. This latter result is a direct consequence of the higher strain of the matrix in these concentrated regions. Surprisingly, the shape of the local concentration distribution does not change qualitatively the results, and quantitatively the effects are quite minor.

References

[1] Lapra A. Etude des mécanismes de renforcement dans les réseaux de élastomères chargés à la silice. Univ. Paris 6. PhD thesis, 1999.
[2] Christensen RM, Lo KH. Solutions for effective shear properties in three phase and cylinder models. J Mech Phys Solids 1979;27:315–30 Erratum 1986;34:639.
[3] Hervé E, Stolz C, Zaoui A. A propos de l'assemblage de sphères composites de Hashin. C R Acad Sci Paris (Serie II) 1991;313(8):857–62.
[4] Stolz C, Zaoui A. Analyse morphologique et approche variationnelles du comportement d'un milieu élastique hétérogène. C R Acad Sci Paris (Serie II) 1991;312(3):143–50.
[5] Burr A. Micromécanique et comportement de matériaux hétérogènes. Univ. Paris 6. PhD thesis. 1995.
[6] Kuhn W, Grün F. Kolloid-Z 1942;101:248.
[7] Treloar LRG. The physics of rubber elasticity. 3rd ed.. Oxford: Clarendon Press, 1975.
[8] Voigt W. Über die Beziehung zwichen den bieden Elastizitätskonstanten isotroper Körper. Wied Ann 1889;38:573.
[9] Bueche F, Halpin JC. J Appl Phys 1964;35:36.
[10] Fedords RF. In: Saltmann WM, editor. The stereo rubbers, New York: Wiley, 1977 chap. 12.
[11] Hutchinson JW. Elastic–plastic behaviour of polycrystalline metals and composites. Proc R Soc London, Series A 1970;319:247–72.
[12] Hutchinson JW. Bounds and self-consistent estimates for creep of polycrystalline materials. Proc R Soc London, Series A 1976;348(1652):101–27.
[13] Hervé E, Zaoui A. Modelling the effective behavior of non-linear matrix/inclusion composites. Eur J Mech A/Solids 1990;9:505–15.
[14] Berveiller M, Zaoui A. An extension of the self-consistent scheme to plastically-flowing polycrystal. J Mech Phys Solids 1979;26:325–44.
[15] Tandon GP, Weng GJ. A theory of particle-reinforced plasticity. J Appl Mech 1988;55(1):126–35.
[16] Weng GJ. The overall elastoplastic stress–strain relations of dual-phase metals. J Mech Phys Solids 1990;38(3):419–41.
[17] Pijaudier-Cabot G, Bazant ZP. Non-local damage theory. J Engng Mech 1987;113:1512.
[18] Ponte Castaneda P. A second-order theory for nonlinear composite materials. CR Acad Sci Paris (Series II) 1996;322(1):3–10.
[19] Hill R. Elastic properties of reinforced solids: some theoretical principles. J Mech Phys Solids 1963;11:357–72.
[20] Eshelby JD. The continuum theory of lattice defects. In: Seitz F, Turnbull D, editors. Solid State Physics, 3. Academic, 1956. p. 79.
[21] Eshelby JD. The determination of the elastic field of an ellipsoidal inclusion and related problems. Proc R Soc London A 1957;241:376–96.
[22] Kerner EH. The elastic and thermo-elastic properties of composite media. Proc Phys Soc B 1956;69:808–13.
[23] Mori T, Tanaka K. Average stress in matrix and average elastic energy of materials with misfitting inclusions. Acta Metall 1973;21(5):571–4.
[24] Nielsen LE. Mechanical properties of polymers and composites, 2. New York: Marcel Dekker, 1974.
[25] Christensen RM. Asymptotic modulus results for composites containing randomly oriented fibers. Int J Solids Struct 1976;12:537–44.
[26] Hill R. A self-consistent mechanics of composite material. J Mech Phys Solids 1965;13:213–22.
[27] Boucher S. On the effective moduli of isotropic two-phase elastic composites. J Comp Mater 1974;8:82–89.
[28] McLaughlin R. A study of the differential scheme for composite materials. Int J Engng Sci 1977;15(4):237–44.

[29] Hervé E, Zaoui A. *n*-Layered Inclusion-based micromechanical modelling. Int J Engng Sci 1993;31(1):1–10.
[30] Reuss A. Berechnung des Fliessgrenze von Mischkristallen auf Grund der Plastizitätbedingung für Einfristalle. Z Angew Math Mech 1929;9:49.
[31] Hashin Z, Shtrikman A. A variational approach to the theory of elastic behavior of multiphase materials. J Mech Phys Solids 1963;11:127–40.
[32] Walpole LJ. J Mech Phys Solids 1966;14:151.
[33] Ponte Castaneda P. The effective mechanical properties of nonlinear isotropic composites. J Mech Phys Solids 1991;39(1):45–71.
[34] Ponte Castaneda P, Suquet P. On the effective mechanical behavior of weakly inhomogeneous nonlinear materials. Eur J Mech A/Solids 1995;14(2):205–36.
[35] Eshelby JD. In: Sneddon IN, Hill R, editors. Progress in solid mechanics, Amsterdam: North-Holland, 1961. p. 89–140.
[36] Hashin Z. The elastic moduli of heterogeneous materials. J Appl Mech 1962;29:143–50.
[37] Bao G, Hutchinson JW, McMeeking RM. The flow stress of dual-phase, non-hardening solids, Mech Mater 1991;12(2):85–94.